Available online at www.sciencedirect.com
ScienceDirect
Bioorganic & Medicinal Chemistry 14 (2006) 8332–8340
Bioorganic & Medicinal Chemistry

Synthesis, enzymatic activity, and X-ray crystallography of an unusual class of amino acids

Wang Chen,[a] Douglas A. Kuntz,[b] Tamika Hamlet,[b] Lyann Sim,[b] David R. Rose[b] and B. Mario Pinto[a,*]

[a]*Department of Chemistry, Simon Fraser University, Burnaby, BC, Canada V5A 1S6*
[b]*Department of Medical Biophysics, University of Toronto and Division of Cancer Genomics and Proteomics, Ontario Cancer Institute, Toronto, Ont., Canada M5G 1L7*

Received 18 July 2006; revised 28 August 2006; accepted 7 September 2006
Available online 28 September 2006

Abstract—The synthesis of two novel amino acids, nitrogen analogues of the naturally occurring glycosidase inhibitor, salacinol, containing a carboxylate inner salt are described, along with the crystal structure of one of these analogues in the active site of *Drosophila melanogaster* Golgi mannosidase II (dGMII). Salacinol, a naturally occurring sulfonium ion, is one of the active principals in the aqueous extracts of *Salacia reticulata* that are traditionally used in Sri Lanka and India for the treatment of diabetes. The synthetic strategy relies on the nucleophilic attack of 2,3,5-tri-*O*-benzyl-1,4-dideoxy-1,4-imino L- or D-arabinitol at the least hindered carbon of 5,6-anhydro-2,3-di-*O*-benzyl-L-ascorbic acid to yield coupled adducts. Deprotection, stereoselective catalytic reduction, and hydrolysis of the coupled products give the target compounds. The compound derived from D-arabinitol inhibits dGMII, one of the critical enzymes in the glycoprotein processing pathway, with an IC_{50} of 0.3 mM. Inhibition of GMII has been identified as a target for control of metastatic cancer. An X-ray crystal structure of the complex of this compound with dGMII provides insight into the requirements for an effective inhibitor. The same compound inhibits recombinant human maltase glucoamylase, one of the key intestinal enzymes involved in the breakdown of glucose oligosaccharides in the small intestine, with a K_i value of 21 μM.

1. Introduction

Glycosidases are involved in several important biological processes, such as digestion, the biosynthesis of glycoproteins, and the catabolism of glycoconjugates.[1] Since glycosidase inhibitors have shown antiviral, insect antifeedant, antidiabetic, and anticancer effects, as well as immune modulatory properties, they have attracted considerable attention. The transition-state structure in the enzyme-mediated hydrolysis of glycosides is believed to be the oxacarbenium ion intermediate with a distorted conformation. Thus, mimicking this distorted, positively charged species is one factor that should lead to an effective inhibitor of glycosidase enzymes.

Many alkaloid sugar mimics with a nitrogen in the ring have been isolated from plants and microorganisms, and inhibit various glycosidases.[2–4] 1-Deoxynojirimycin (**1**), which is a D-glucose analogue with an NH group in place of the ring oxygen atom, has been shown to inhibit intestinal α-glucosidases and pancreatic α-amylase both in vitro and in vivo, as well as α-glucosidases I and II involved in N-linked oligosaccharide processing.[5] Two N-alkylated analogues of deoxynojirimycin, namely miglitol (**2**) and *N*-butyldeoxynojirimycin (**3**), are currently in use as drugs for the treatment of Type II diabetes and Gaucher's disease, respectively. Both drugs act by inhibition of glucosidase enzymes. 1,4-Dideoxy-1,4-imino-D-arabinitol (D-AB1) (**4**), which was first isolated from the fruits of the legume *Angylocalyx boutiquenus*, was found to be a potent inhibitor of hepatic glycogen phosphorylase.[6] Its synthetic L-enantiomer (L-AB1) (**5**) is a powerful inhibitor of mammalian α-D-glucosidases.[7,8] The naturally occurring glycosidase inhibitor acarbose (**6**),[9] which contains a nitrogen atom in one of the linkages between the

Keywords: Glycosidase inhibitors; Salacinol; Nitrogen analogues; Carboxylate counterions; Amino acids; Iminoarabinitols; Epoxide; Amino acids; L-Ascorbic acid; Stereoselective catalytic reduction; Golgi mannosidase II; Human maltase glucoamylase.
* Corresponding author. Tel:. +1 604 291 4152; fax: +1 604 291 4860; e-mail: bpinto@sfu.ca

0968-0896/$ - see front matter © 2006 Published by Elsevier Ltd.
doi:10.1016/j.bmc.2006.09.004

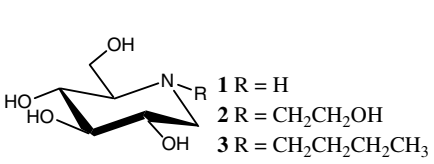

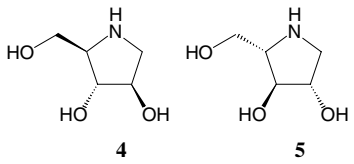

4 5

sugar and pseudosugar units, is the highest-affinity carbohydrate analogue for a binding protein and has also been used for the treatment of type-2 diabetes.[10,11] It is generally believed that this strong binding originates from electrostatic interactions of the positively charged, protonated nitrogen atom with carboxylate residues in the enzyme active site.[5]

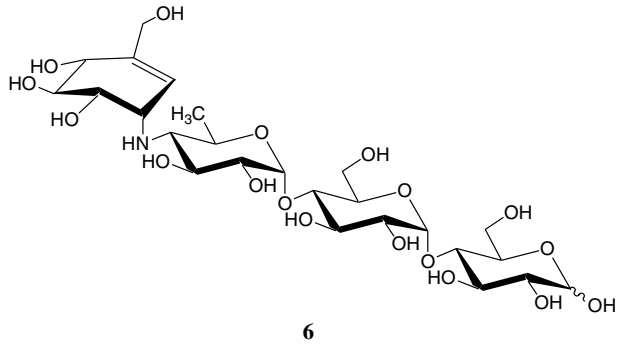

6

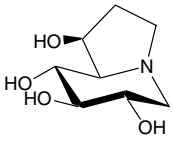

7

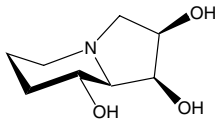

8

A similar mode of action has been suggested for the naturally occurring indolizidine alkaloids castanospermine (**7**) and swainsonine (**8**).

Sulfonium-ion mimics of the oxacarbenium ion contain a permanent positive charge, which could make strong interactions with the active-site carboxylate residues. The most interesting glycosidase inhibitors in the form of cyclic sulfonium ions are perhaps the naturally occurring compounds salacinol (**9**) and kotalanol (**10**).[12,13] The α-glucosidase inhibitory activity of salacinol was confirmed to be as strong as that of acarbose, which is used clinically.[14] The zwitterionic structure of salacinol is unique in that a negative charge is positioned at the sulfate group and the positive charge is centered at the sulfur atom.[12] Molecular dynamics simulations have shown that enzyme charge distribution plays an important role in guiding charged ligands to the active site of *Torpedo californica* acetylcholinesterase.[15] Zhou et al. have shown that the electrostatic potential within the active site can be used to predict the electrostatic rate enhancement for acetylcholinesterase-substrate binding.[16] Of note, zwitterionic inhibitors have been predicted to bind to a neuraminidase enzyme more effectively than the singly charged, anionic species.[17] Thus, the zwitterionic salacinol should be quite different from conventional glycosidase inhibitors which mimic just the positive charge of the transition state. Structural modification of salacinol represents a promising approach in the search for new glycosidase inhibitors. One strategy is to replace the sulfur atom in salacinol with a nitrogen atom, and we have reported the synthesis of nitrogen analogues (**11** and **12**) of salacinol and their evaluation as glycosidase inhibitors.[18] Compound **11** also selectively inhibits the lysosomal α-glucosidases.[19]

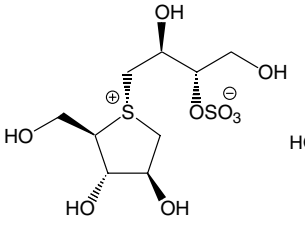

9

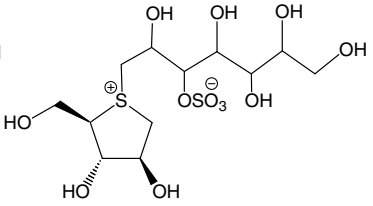

10

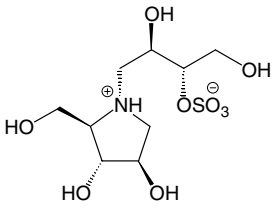

11

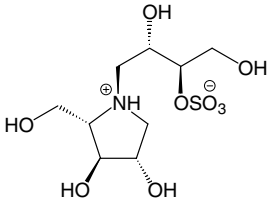

12

The fact that salacinol has greater inhibitory activity and specificity against α-glucosidases than the methyl sulfonium ion (**13**) indicates that the sulfate group is important.[20] Yuasa et al.[21] reported that docking of salacinol into the binding site of glucoamylase indicated close contacts between the sulfate ion with Arg305. Crystallographic analysis of the interactions of *Drosophila melanogaster* Golgi α-mannosidase II (dGMII) with salacinol and its analogues shows that the sulfate group does interact with residues in the enzyme active site.[22] Compound **14**, isolated from a marine sponge in Japan, was also reported to be a strong inhibitor of α-glucosidase.[23] The sulfate groups in **14** may play a role similar to that proposed for the sulfate group of salacinol.[21]

An intriguing question is whether the corresponding carboxylate analogues of salacinol will act as inhibitors of glucosidases. We now report the synthesis of novel amino acids that are nitrogen analogues (**15** and **16**) of salacinol containing a carboxylate inner salt.

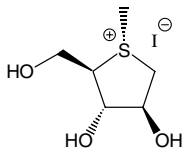

13

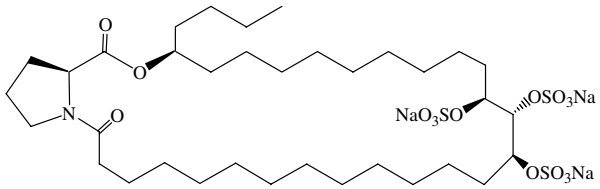

14

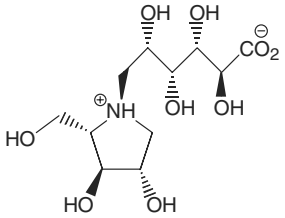

15

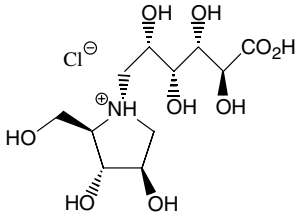

16

2. Results and discussion

2.1. Synthesis

Retrosynthetic analysis indicated that amino acids **A** could be obtained by alkylation of the iminoarabinitols **B** at the nitrogen atom (Scheme 1). The alkylating agent could be an epoxide **C**, whereby regioselective attack of the amine at the least hindered primary center should afford the desired amino acids.[24] The epoxide **C** could be synthesized from inexpensive vitamin C (**D**).

The epoxide **20** was synthesized using a simplified procedure of Raic-Malic et al. (Scheme 2).[25] The iminoarabinitols **23** and **26** were synthesized from D-xylose and L-xylose, respectively, following a similar strategy that has been described previously in the literature (Scheme 3).[26–28]

Coupling of 2,3,5-tri-*O*-benzyl-1,4-dideoxy-1,4-imino-L-arabinitol **23** with the benzyl-protected L-ascorbic acid epoxide **20** in dry acetonitrile at 70 °C gave the protected compound **27** in 82% yield (Scheme 4). No side products were obtained. Debenzylation of the coupled product **27** by hydrogenolysis and subsequent stereoselective catalytic reduction of the C4′–C5′ double bond of the L-ascorbic acid moiety, using a widely employed procedure,[29–31] afforded **28**. Catalytic hydrogenation of the L-ascorbic acid was reported to proceed with complete diastereoselectivity.[29,30] The reduction of the double bond in **27** was monitored by MALDI-TOF mass spectrometry as a hydrogen chloride salt. Even though a high pressure of H_2 was used, the reduction was complete only after 4 days. Without further purification, the crude compound **28** was treated with aqueous potassium carbonate. After hydrolysis of the lactone ring in **28** and neutralization of potassium carbonate with acid, the resulting inorganic salts were removed using Sephadex G-10 chromatography to yield **15**. The overall yield for the two steps was 78%. The structure of the zwitterion **15** was confirmed by MALDI-TOF mass spectrometry, microanalysis data, and ^{1}H and ^{13}C NMR spectroscopy.

Compound **16**, the diastereomer of **15**, was similarly obtained by reaction of the amine **26** with the epoxide **20** to produce the protected compound **29** in 74% yield (Scheme 5). Deprotection, stereoselective catalytic reduction, and hydrolysis, and exchange of Na^{+} ion with excess cation-exchange resin gave compound **16** in 62% yield. In this case, the compound was obtained as a chloride salt, as confirmed by MALDI-TOF mass spectrometry, microanalysis data, and ^{1}H and ^{13}C NMR spectroscopy.

NMR spectra were performed on samples of compounds **15** and **16** in deuterated water, made basic with small amounts of sodium deuteroxide to give the corresponding amines, to ensure the peaks were more defined. We believe that the broadening of the peaks in the absence of base is due to chemical exchange between the ammonium salts and the corresponding tertiary amines, a process that is in the intermediate-exchange regime on the NMR time scale. In the presence of base, only the rapidly inverting tertiary amines are present, and conformationally averaged NMR spectra in the fast-exchange regime are observed.

2.2. Enzyme inhibitory activity

We measured the enzyme inhibitory activity of the amino acids **15** and **16**. Compound **16** inhibits recombinant human maltase glucoamylase (MGA), a critical

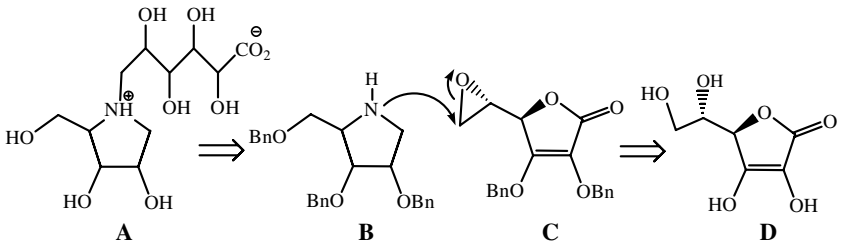

Scheme 1.

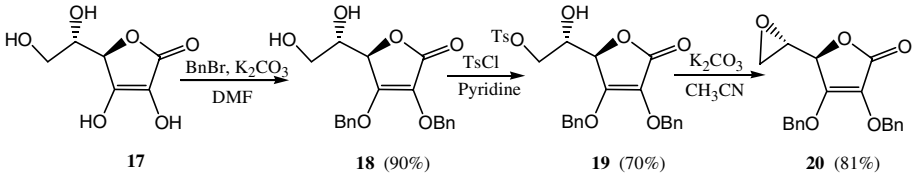

Scheme 2.

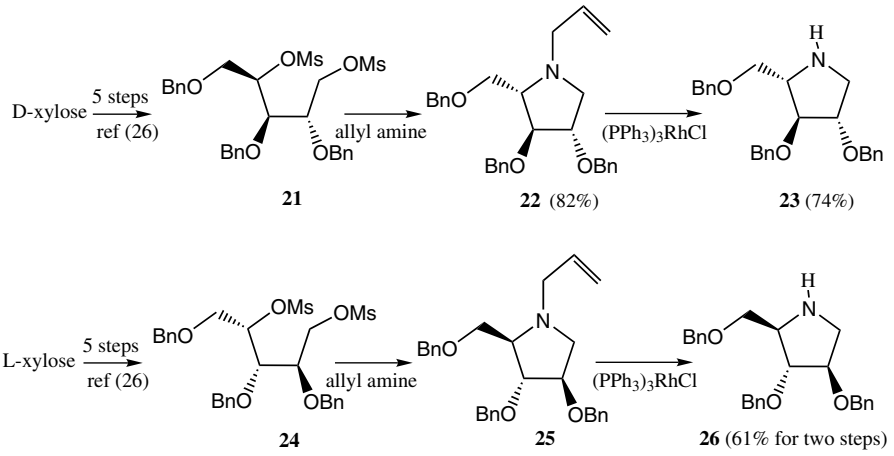

Scheme 3.

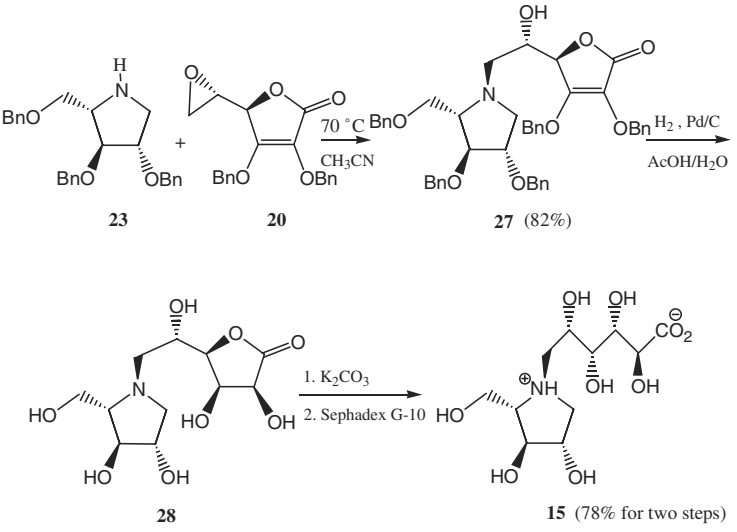

Scheme 4.

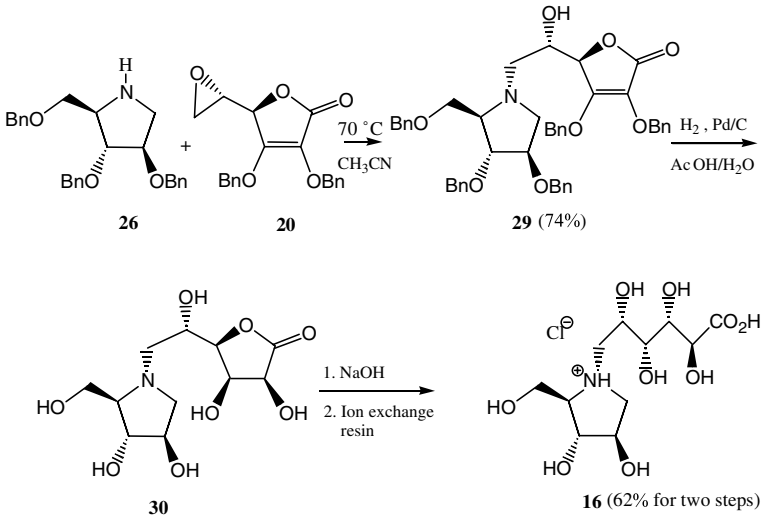

Scheme 5.

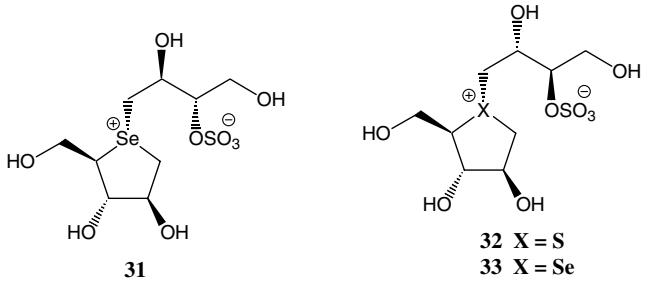

Scheme 6.

intestinal glucosidase involved in the processing of oligosaccharides of glucose into glucose itself, with a K_i value of 21 μM. Salacinol itself has a K_i value of 0.2 μM. Compound **16** is also active against *Drosophila melanogaster* Golgi α-mannosidase II (dGMII) with an IC_{50} of 0.3 mM. This is a significant improvement (25-fold) over the inhibition measured for other salacinol analogues which all inhibited dGMII with an IC_{50} of approximately 7.5 mM (**9**, **11**, **31**–**33**, Scheme 6).[22] Compound **15** is not active on either enzyme; similar results were obtained for other salacinol analogues derived from anhydro-L-heteroarabinitol moieties and presumably reflect minimal contacts of the enantiomeric five-membered rings in the enzyme active sites.[18,22]

2.3. X-ray crystallography

We have solved the crystal structure of **16** bound in the active site of dGMII. Statistics for data collection and refinement are presented in Table 1. The electron density of the bound compound **16** is shown in Figure 1. Close interactions (with a distance of less than 3.2 Å) are highlighted in Figure 2 and the corresponding distances in comparison with the nanomolar inhibitor swainsonine are detailed in Table S1 (Supporting information).

Table 1. Statistics for data collection and refinement

PDB code/HET symbol	2FYV/W72
Space Group	$P2_12_12_1$
Cell dimensions (Å)	68.81 × 108.64 × 137.38
Data collection (values in parentheses represent high resolution shell)	
Resolution (Å)	30–1.90 (1.95–1.90)
Unique reflections/redundancy	81152/5.7 (5388/2.7)
I/sigma *I*	12.4 (2.5)
% completeness	99.6 (95.4)
R merge	0.092 (0.41)
Wilson B ($Å^2$)	13.3
Structure refinement	
R_{workt}/R_{free} (reflections for R_{free})	0.162/0.212 (1848)
Amino acids/alternate conformers	1044/10
Water molecules/heteroatoms	1048/49
rmsd bonds (Å)/rmsd angles (°)	0.2/1.9
Average B factors ($Å^2$)	
Overall	16.8
Protein main chain/side chain	14.5/16.4
Water	26.7
Inhibitor (range)	25.6(10–44)
Zn/MPD/PO_4	10.8/21.4/42.9

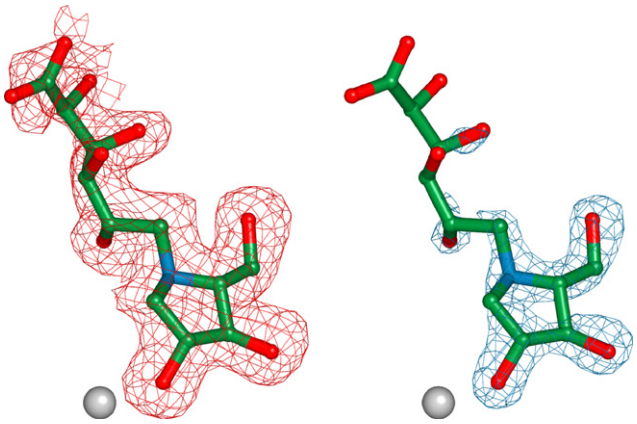

Figure 1. Stereoview of **16** in the active site of *Drosophila melanogaster Golgi* mannosidase II and its surrounding electron density. The electron density was determined as a simulated annealing omit map ($F_o - F_c$) and is contoured at 2 sigma (red) or 5 sigma (blue). The active-site zinc ion is shown in gray.

Similar to the other salacinol analogues (and in contrast to most other inhibitors bound to dGMII) only a single hydroxyl group (OH2) interacts with the active-site zinc atom. Also, as seen in other salacinol analogues, Tryptophan95 stacks on top of the ring portion of **16**, and the ring hydroxyl groups form hydrogen bonds with aspartate residues (D92, D204, and D472 with OH1 and D472 with OH2) and tyrosine (Y727 OH with OH2). The C6 OH forms hydrogen bonds with the carbonyl oxygen of R876 as well as a bound water molecule. D204 makes a hydrogen bond with the nitrogen atom of compound **16**.

It is in the acyclic chain of **16** that the interactions of the inhibitor exhibit the most significant differences from the other salacinol analogues, and it is these novel interactions which may account for the increased potency of **16** in comparison to its parent compound **11**. The hydroxyl groups of this chain form extensive contacts with both side chains and water molecules in the active site. The electron density in this region is more ill defined than that of the ring region and this indicates that there is mobility of the chain. Flexibility of this region is also reflected in the temperature (B) factors which are a measure of atomic mobility. B-factors in the ring region are in the range of 10–15 $Å^2$ (the zinc bound OH1 is below 10 $Å^2$) while those in the tail region approach 44 $Å^2$.

Hydrogen bonds in the acyclic region occur between O8 and the catalytic nucleophile D204, as well as R228 and Y269. O9 interacts with the acid–base catalyst residue D341 and two waters. O11 hydrogen bonds to one water while O12 makes close contacts with two waters. The carbonyl O13 interacts with D340 and 2 water molecules, one of which is shared with O9 and the other shared with O12, D340 and D270.

Figure 3A shows an overlay of **16** (this work) and swainsonine (from PDB 1HWW) bound in the crystal structure of dGMII. Although the reason for the potency of swainsonine has not been clearly determined, it is one of the best inhibitors of dGMII, with an IC_{50} value in the range of 20–40 nM, and is believed to closely mimic the oxacarbenium ion which occurs in the reaction pathway. The position of the nitrogen moiety, which is designed to serve as the mimic of the positive charge on the oxacarbenium ion, is almost identical in the two bound structures. However, in contrast with swainsonine, only a single hydroxyl group of **16** is in contact with the active site zinc ion. As well, the orientation of the second hydroxyl group, which forms hydrogen bonds with

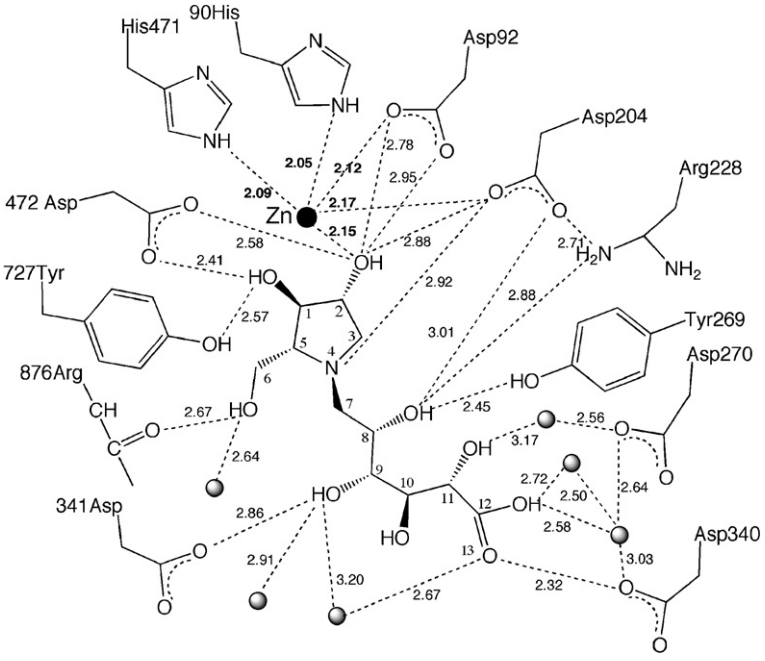

Figure 2. Interactions of compound **16** with *Drosophila* GMII. Only interactions less than 3.2 Å are indicated. The zinc ion in the active site is depicted as a black ball and water molecules are shown as gray spheres. Distances are given in Angstrom units. Numbering of the inhibitor is as it occurs in the PDB file.

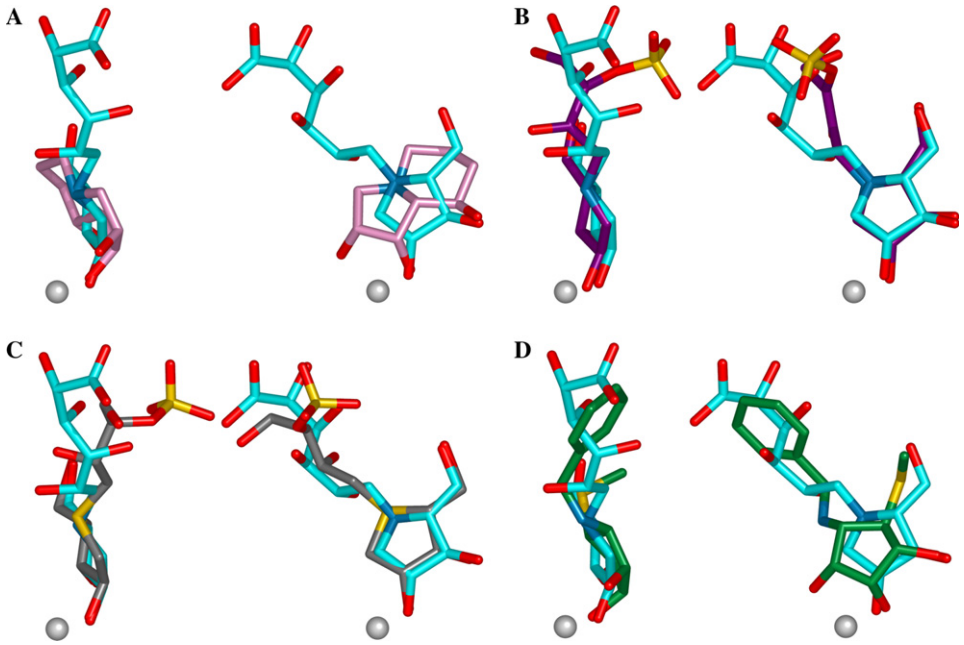

Figure 3. Overlay of compounds bound in the active site of dGMII. Compound **16** (cyan) is overlaid with **A**. Swainsonine (pink, PDB 1HWW) **B**. Ghavamiol **11** (magenta, PDB 1TQU) **C**. Salacinol diastereomer **32** (gray, PDB 1TQT) or **D**. *N*-Benzyl mannostatin (green, PDB 2F7P).

D472 and Y727, differs in the two structures, and it is possible that this geometry is not ideal for forming strong interactions. While the position of the head group of **16** is comparable to those of the other salacinol analogues[22] the region of space occupied by the acyclic tail region is quite different. Figure 3 shows overlays of **16** bound in the crystal structure of dGMII with bound ghavamiol **11** (Fig. 3B) or the diastereomer of salacinol **32** (Fig. 3C) solved previously (PDBs 1TQU and 1TQT[22]). In both cases the position of the sulfate group is quite different from that of the carboxyl group, and the space through which the aliphatic chain passes is also quite different. Interestingly, the region of the active site through which the aliphatic chain of **16** passes is very much comparable to that of a recently solved benzyl-mannostatin A–dGMII complex.[32] The overlay of the two complexes (Fig. 3D) shows them to intertwine, although the nature of the interactions formed by the two tail moieties is different. The benzyl tail reduced the potency of the mannostatin to which it was attached[33], while in the present case the carboxylate tail greatly increased the inhibitory activity of the salacinol head group. Given the much better inhibitory properties of the mannostatin derivatives (nM) in comparison to the salacinol derivatives (mM) it is possible that attachment of a similar carboxylate tail to a mannostatin head group would lead to a very effective mannosidase inhibitor.

3. Experimental

3.1. Enzyme activity assays

Measurement of dGMII inhibition was carried out as outlined previously.[22] Analysis of recombinant MGA inhibition and determination of the kinetic constants for competitive inhibition have been described.[34] Briefly, analysis of MGA inhibition was performed using maltose as the substrate and measuring the release of glucose. Reactions were carried out in 100 mM Mes buffer, pH 6.5, at 37 °C. The reaction was stopped by boiling for 3 min. Twenty microliter aliquots were taken and added to 100 μL of glucose oxidase assay reagent (Sigma) in a 96-well plate. Reactions were developed for 1 h and absorbance was measured at 450 nm to determine the amount of glucose produced by MGA activity in the reaction. All reactions were performed in triplicate and absorbance measurements were averaged to give a final result.

3.2. Enzyme kinetics

Kinetic parameters of recombinant MGA were determined using the glucose oxidase assay to follow the production of glucose upon addition of enzyme (15 nM) at increasing maltose concentrations (from 2.5 to 30 mM) with a reaction time of 15 min. The K_i value was determined by measuring the rate of maltose hydrolysis by MGA at varying inhibitor concentrations. Data were plotted in Lineweaver–Burk plots (1/rate vs 1/[substrate]) and the K_i value was determined by the equation $K_i = K_m[I]/(V_{max})s - K_m$, where '$s$' is the slope of the line. The K_i reported was an average of the K_i values obtained from each of the different inhibitor concentrations.

3.3. Structure determination of dGMII–16 complex

Preparation of dGMII crystals soaked with **16** was carried out essentially as described previously.[22] In this case however, the crystals were first washed with reservoir buffer containing phosphate instead of Tris, to reduce any effects of Tris binding in the active site. The crystals were soaked for 24 h with a 2 mM solution of **16** in phosphate containing reservoir buffer. The crystals were

passed through phosphate-buffered cryo-solutions containing 1 mM inhibitor prior to rapid freezing in a liquid nitrogen stream. X-ray diffraction data were collected at 100 K with a Bruker X8 Proteum system consisting of a CCD detector and a Bruker Microstar rotating anode generator. Data were integrated and scaled using the Proteum suite of programs (Bruker AXS, Madison WI). Structure solution and refinement were carried out using the programs CNS[35] and O[36] as previously described.[22] Diagrams were rendered in Pymol.[37]

3.4. *N*-Allyl-2,3,5-tri-*O*-benzyl-1,4-dideoxy-1,4-imino-L-arabinitol (22), *N*-allyl-2,3,5-tri-*O*-benzyl-1,4-dideoxy-1,4-imino-D-arabinitol (25), 2,3,5-tri-*O*-benzyl-1,4-dideoxy-1,4-imino-L-arabinitol (23), 2,3,5-tri-*O*-benzyl-1,4-dideoxy-1,4-imino-D-arabinitol (26)

Compounds **22**, **23**, **25**, and **26** were synthesized according to the original literature procedures.[26–28]

3.5. 6′-((2,3,5-Tri-*O*-benzyl-1,4-dideoxy-1,4-imino-L-arabinitol)-4-*N*-yl)-2′,3′-di-*O*-benzyl-6′-deoxy-L-ascorbic acid (27)

A mixture of 2,3,5-tri-*O*-benzyl-1,4-dideoxy-1,4-imino-L-arabinitol **23** (404 mg, 1.0 mmol) and 5,6-anhydro-2,3-di-*O*-benzyl-L-ascorbic acid **20** (340 mg, 1.0 equiv) was dissolved in dry CH_3CN (5 mL). The mixture was stirred in a round-bottomed flask in an oil-bath (70 °C) overnight. The solvent was removed under reduced pressure, and the product was purified by column chromatography (hexanes–EtOAc, 3:1) to afford **27** (612 mg, 82%) as a yellow oil. $[\alpha]_D$ +23° (*c* 0.6, CH_2Cl_2). ^1H NMR ($CDCl_3$): δ 7.11–7.30 (25H, m, Ar), 5.12 and 5.04 (2H, 2d, $J_{A,B}$ = 11.8 Hz, C=C–OCH_2Ph), 5.01 and 4.98 (2H, 2d, $J_{A,B}$ = 11.3 Hz, C=C–OCH_2Ph), 4.57 (1H, d, $J_{2',3'}$ = 1.5 Hz, H-3′), 4.44 and 4.42 (2H, 2d, $J_{A,B}$ = 6.3 Hz, CH_2Ph), 4.39 and 4.36 (2H, 2d, $J_{A,B}$ = 9.4 Hz, CH_2Ph), 4.35 and 4.33 (2H, 2d, $J_{A,B}$ = 12.0 Hz, CH_2Ph), 3.89 (1H, ddd, $J_{1a,2}$ = 1.6 Hz, $J_{1b,2}$ = 5.5 Hz, $J_{2,3}$ = 1.8 Hz, H-2), 3.84 (1H, ddd, $J_{1'a,2'}$ = 8.0 Hz, $J_{1'b,2'}$ = 6.0 Hz, H-2′), 3.76 (1H, dd, $J_{3,4}$ = 3.9 Hz, H-3), 3.46 (1H, dd, $J_{4,5a}$ = 5.9 Hz, $J_{5a,5b}$ = 9.8 Hz, H-5a), 3.43 (1H, dd, $J_{4,5b}$ = 5.9 Hz, H-5b), 3.09 (1H, dd, $J_{1a,1b}$ = 10.5 Hz, H-1a), 2.88 (1H, dd, $J_{1'a,1'b}$ = 13.0 Hz, H-1′a), 2.84 (1H, dt, H-4), 2.77 (1H, dd, H-1b), 2.73 (1H, dd, H-1′b). ^{13}C NMR ($CDCl_3$): δ 169.57 (C-6′), 157.44 (C-4′), 137.86, 137.79, 137.73, 135.85, 135.32 (5C_{ipso}), 128.76–127.24 (25C_{Ar}), 120.68 (C-5′), 84.59 (C-3), 81.63 (C-2), 75.54 (C-3′), 73.60 and 72.98 (2C=C–OCH_2Ph), 72.87, 71.09, 70.78 (3CH_2Ph), 70.34 (C-5), 68.95 (C-4), 66.93 (C-2′), 58.00 (C-1), 56.69 (C-1′). MALDI-TOF MS: *m/e* 763.85 (M^++Na), 742.075 (M^++H). Anal. Calcd for $C_{46}H_{47}O_8N$: C, 74.43; H, 6.38; N, 1.89. Found: C, 74.20; H, 6.35; N, 2.14.

3.6. 6′-((1,4-Dideoxy-1,4-imino-L-arabinitol)-4-*N*-ammonium)-6′-deoxy-L-gulonate (15)

The protected compound **27** (300 mg, 0.4 mmol) was dissolved in AcOH–H_2O (4:1, 6 mL) and stirred with Pd/C (30 mg) under H_2 (70 psi). After 4 days, the reaction mixture was filtered through a cotton, which was subsequently washed with H_2O. The combined filtrates were concentrated under vacuum. Concentrated hydrochloric acid (1 mL) was added and the mixture was concentrated by high vacuum. The obtained solid was dissolved in aqueous K_2CO_3 solution (1 mL, pH 9.0) and the mixture was stirred for 3 h. The solution was neutralized with dilute hydrochloric acid and then concentrated. The residue was purified by Sephadex G-10 chromatography column to give **15** as an amorphous solid (104 mg, 78%). $[\alpha]_D$ +10° (*c* 0.1, H_2O). ^1H NMR (D_2O, pH = 12.0): δ 4.03 (1H, d, $J_{4',5'}$ = 4.5 Hz, H-5′), 3.98 (1H, br d, H-2), 3.83 (1H, d, H-4′), 3.79 (2H, br d, H-3, H-2′), 3.64 (1H, m, H-3′), 3.61 (2H, m, 2H-5), 2.99 (1H, d, $J_{1a,1b}$ = 11.1 Hz, H-1a), 2.91 (1H, dd, $J_{1'a,1'b}$ = 12.8 Hz, $J_{1'a,2'}$ = 5.0 Hz, H-1′a), 2.73 (1H, dd, $J_{1b,2}$ = 5.0 Hz, H-1b), 2.47 (1H, m, H-4), 2.43 (1H, dd, $J_{1'b,2}$ = 7.1 Hz, H-1′b). ^{13}C NMR (D_2O, pH 12.0): δ 179.13 (C-6′), 76.50 (C-3), 73.35 (C-2), 71.45 (C-5′), 70.27 (C-4′), 69.86 (C-4), 69.35 (C-3′), 68.39 (C-2′), 58.46 (C-5), 57.44 (C-1), 54.98 (C-1′). MALDI-TOF MS: *m/e* 334.47 (M^++Na), 312.43 (M^++H). Anal. Calcd for $C_{11}H_{21}O_9N$: C, 42.44; H, 6.80; N, 4.50. Found: C, 42.19; H, 6.66; N, 4.36.

3.7. 6′-((2,3,5-Tri-*O*-benzyl-1,4-dideoxy-1,4-imino-D-arabinitol)-4-*N*-yl)-2′,3′-di-*O*-benzyl-6′-deoxy-L-ascorbic acid (29)

A mixture of 2,3,5-tri-*O*-benzyl-1,4-dideoxy-1,4-imino-D-arabinitol **26** (444 mg, 1.1 mmol) and 5,6-anhydro-2,3-di-*O*-benzyl-L-ascorbic acid **20** (374 mg, 1.0 equiv) was dissolved in dry CH_3CN (5 mL). The mixture was stirred in a round-bottomed flask in an oil-bath (70 °C) overnight. The solvent was removed under reduced pressure, and column chromatography (hexanes–EtOAc, 3:1) of the crude product gave **29** (605 mg, 74%) as a yellow oil. $[\alpha]_D$ +6° (*c* 0.7, CH_2Cl_2). ^1H NMR ($CDCl_3$): δ 7.13–7.30 (25H, m, Ar), 5.22 and 5.04 (2H, 2d, $J_{A,B}$ = 11.7 Hz, C=C–OCH_2Ph), 5.11 and 5.05 (2H, 2d, $J_{A,B}$ = 11.3 Hz, C=C–OCH_2Ph), 4.51 (1H, br d, H-3′), 4.50–4.40 (6H, m, 3CH_2Ph), 3.96 (1H, dt, $J_{1a,2}$ = 1.7 Hz, $J_{1b,2}$ = 5.5 Hz, H-2), 3.88 (1H, dd, $J_{2,3}$ = 1.8 Hz, $J_{3,4}$ = 4.4 Hz, H-3), 3.87 (1H, m, H-2′), 3.53 (1H, dd, $J_{4,5a}$ = 5.3 Hz, $J_{5a,5b}$ = 9.8 Hz, H-5a), 3.51 (1H, dd, $J_{4,5b}$ = 5.6 Hz, H-5b), 3.23 (1H, d, $J_{1a,1b}$ = 10.4 Hz, H-1a), 3.17 (1H, dd, $J_{1'a,1'b}$ = 12.5 Hz, $J_{1'a,2'}$ = 10.9 Hz, H-1′a), 2.88 (1H, q, H-4), 2.64 (1H, dd, H-1b), 2.52 (1H, dd, $J_{1'b,2'}$ = 3.5 Hz, H-1′b). ^{13}C NMR ($CDCl_3$): δ 169.90 (C-6′), 157.43 (C-4′), 138.24, 138.21, 138.19, 136.36, 135.80 (5C_{ipso}), 128.96-127.64 (25C_{Ar}), 121.22 (C-5′), 84.83 (C-3), 82.03 (C-2), 75.94 (C-3′), 74.20 and 73.62 (2C=C–OCH_2Ph), 73.49, 71.79, 71.38 (3CH_2Ph), 70.28 (C-5), 69.12 (C-4), 66.28 (C-2′), 57.40 (C-1), 57.10 (C-1′). MALDI-TOF MS: *m/e* 764.03 (M^++Na), 741.95 (M^++H). Anal. Calcd for $C_{46}H_{47}O_8N$: C, 74.43; H, 6.38; N, 1.89. Found: C, 74.27; H, 6.39; N, 2.03.

3.8. 6′-((1,4-Dideoxy-1,4-imino-D-arabinitol)-4-*N*-ammonium)-6′-deoxy-L-gulonic acid hydrochloride (16)

The protected compound **29** (600 mg, 0.8 mmol) was dissolved in AcOH–H_2O (4:1, 10 mL) and stirred with Pd/C (50 mg) under H_2 (70 psi). After 4 days, the reaction mixture was filtered through cotton, which was sub-

sequently washed with H_2O. The combined filtrates were concentrated under vacuum. Concentrated hydrochloric acid (2 mL) was added and the mixture was concentrated by high vacuum. The obtained solid was dissolved in aqueous NaOH solution (2 mL, pH 9.0) and the mixture was stirred for 3 h. The solution was neutralized with dilute hydrochloric acid. Na^+ ion was removed with excess Amberlite IR-120-P (H^+ form) and the resin was removed by filtration. The aqueous solution was concentrated to give **16** as an amorphous solid (165 mg, 62%). $[\alpha]_D$ +2° (*c* 0.5, H_2O). ^1H NMR (D_2O, pH 12.0): δ 3.94 (1H, d, $J_{4',5'} = 4.8$ Hz, H-5′), 3.89 (1H, m, H-2), 3.75–3.71 (3H, m, H-4′, H-3, H-2′), 3.57–3.52 (2H, m, 2H-5), 3.50 (1H, m, H-3′), 2.90 (1H, dd, $J_{1a,1b} = 10.4$ Hz, $J_{1a,2} = 1.1$ Hz, H-1a), 2.76 (1H, dd, $J_{1'a,1'b} = 13.0$ Hz, $J_{1'a,2'} = 9.4$ Hz, H-1′a), 2.57 (1H, dd, $J_{1b,2} = 5.6$ Hz, H-1b), 2.36 (1H, m, H-1′b), 2.33 (1H, m, H-4); ^{13}C NMR (D_2O, pH 12.0): δ 179.00 (C-6′), 79.24 (C-3), 75.95 (C-2), 74.18 (C-5′), 72.71 (C-4′), 72.30 (C-4, C-3′), 70.06 (C-2′), 60.70 (C-5), 58.99 (C-1), 57.54 (C-1′). MALDI-TOF MS: *m/e* 334.52 (M^++Na), 312.32 (M^++H). Anal. Calcd for $C_{11}H_{22}O_9NCl$: C, 38.00; H, 6.37; N, 4.03. Found: C, 38.15; H, 6.45; N, 3.86.

Acknowledgments

We are grateful to Blair D. Johnston for helpful discussion and to the Natural Sciences and Engineering Research Council of Canada and the Canadian Institutes for Health Research for financial support.

Supplementary data

Details of X-ray crystal structure determination, Table comparing interatomic distances in *Drosophila* Golgi mannosidase II (1 page), and CIF file. Supplementary data associated with this article can be found, in the online version, at doi:10.1016/j.bmc.2006.09.004.

References and notes

1. For leading references Dwek, R. A. *Chem. Rev.* **1996**, *96*, 683–720; *Essentials of Glycobiology*; Varki, A., Cumming, R., Esko, J., Freeze, H., Hart, G., Marth, J., Eds.; Cold Spring Harbor Laboratory Press: Cold Spring Harbor, NY, 1999.
2. Elbein, A. D. *Annu. Rev. Biochem.* **1987**, *56*, 497–534.
3. Fellows, L. E.; Kite, G. C.; Nash, R. J.; Simmonds, M. S. J.; Scofield, A. M. Castanospermine, Swainsonine, and Related Polyhydroxy Alkaloids: Structure, Distribution and Biological Activity. In *Plant Nitrogen Metabolism*; Poulton, J. E., Romero, J. T., Conn, E. E., Eds.; Plenum: New York, 1989; pp 395–427.
4. Legler, G. *Adv. Carbohydr. Chem. Biochem.* **1990**, *48*, 319–384.
5. *Iminosugars as Glycosidase Inhibitors: Nojirimycin and Beyond*; Stutz, A. E., Ed.; Wiley-VCH: Weinheim: New York, 1999.
6. Fosgerau, K.; Westergaard, N.; Quistorff, B.; Grunner, N.; Kristiansen, M.; Lundgren, K. *Arch. Biochem. Biophys.* **2000**, *380*, 274–284.
7. Fleet, G. W. J.; Nicholas, S. J.; Smith, P. W. *Tetrahedron Lett.* **1985**, *26*, 3127–3130.
8. Scofield, A. M.; Fellows, L. E.; Nash, R. J.; Fleet, G. W. J. *Life Sci.* **1986**, *39*, 645–650.
9. Bock, K.; Sigurskjold, B. *Stud. Nat. Prod. Chem* **1990**, *7*, 29–86.
10. Holman, R. R.; Cull, C. A.; Turner, R. C. *Diabetes Care* **1999**, *22*, 960–964.
11. Jacob, G. S. *Curr. Opin. Struct. Biol.* **1995**, *5*, 605–611.
12. Yoshikawa, M.; Murakami, T.; Shimada, H.; Matsuda, H.; Yamahara, J.; Tanabe, G.; Muraoka, O. *Tetrahedron Lett.* **1997**, *38*, 8367–8370.
13. Yoshikawa, M.; Murakami, T.; Yashiro, K.; Matsuda, H. *Chem. Pharm. Bull.* **1998**, *46*, 1339–1340.
14. Asano, N. *Glycobiology* **2003**, *13*(10), 93R–104R.
15. Antosiewicz, J.; Wlodek, S. T.; McCammon, J. A. *Biopolymers* **1996**, *39*, 85–94.
16. Zhou, H.-X.; Briggs, J. M.; McCammon, J. A. *J. Am. Chem. Soc.* **1996**, *118*, 13069–13070.
17. Bonnet, P.; Bryce, R. A. *Protein Sci.* **2004**, *13*, 946–957.
18. Ghavami, A.; Johnston, B. D.; Jensen, M. T.; Svensson, B.; Pinto, B. M. *J. Am. Chem. Soc.* **2001**, *123*, 6268–6271.
19. Li, Y.; Scott, C. R.; Chamoles, N. A.; Ghavami, A.; Pinto, B. M.; Turecek, F.; Gelb, M. H. *Clin. Chem.* **2004**, *50*, 1785–1796.
20. Yuasa, H.; Takada, J.; Hashimoto, H. *Bioorg. Med. Chem. Lett.* **2001**, *11*, 1137–1139.
21. Yuasa, H.; Saotome, C.; Kanie, O. *Trends Glycosci. Glycotechnol.* **2002**, *14*, 231–251.
22. Kuntz, D. A.; Ghavami, A.; Johnston, B. D.; Pinto, B. M.; Rose, D. R. *Tetrahedron: Asymmetry* **2005**, *16*, 25–32.
23. Nakano, Y.; Maki, T.; Matsunaga, S.; van Soest, R. W. M.; Fusetani, N. *Tetrahedron* **2000**, *56*, 8977–8987.
24. Efange, S. M. N.; Michelson, R. H.; Dutta, A. K.; Parsons, S. M. *J. Med. Chem.* **1991**, *34*, 2638–2643.
25. Raic-Malic, S.; Svedruzic, D.; Gazivoda, T.; Marunovic, A.; Hergold-Brundic, A.; Nagl, A.; Balzarini, J.; De Clercq, E.; Mintas, M. *J. Med. Chem.* **2000**, *43*, 4806–4811.
26. Satoh, H.; Yoshimura, Y.; Sakata, S.; Miura, S.; Machida, H. *Bioorg. Med. Chem. Lett.* **1998**, *8*, 989–992.
27. Veerapen, N.; Yuan, Y.; Sanders, D. R. A.; Pinto, B. M. *Carbohydr. Res.* **2004**, *339*, 2205–2217.
28. Overkleeft, H. S.; Wiltenburg, J.; Pandit, U. K. *Tetrahedron* **1994**, *50*, 4215–4224.
29. Czarnocki, Z.; Mieczkowski, J. B.; Ziolkowski, M. *Tetrahedron: Asymmetry* **1996**, *7*, 2711–2720.
30. Andrews, G. C.; Crawford, T. C.; Bacon, B. E. *J. Org. Chem.* **1981**, *46*, 2976–2977.
31. Joseph, C. C.; Regeling, H.; Zwanenburg, B.; Chittenden, G. J. F. *Tetrahedron* **2002**, *58*, 6907–6912.
32. Kawatkar, S. P.; Kuntz, D. A.; Woods, R. J.; Rose, D. R.; Boons, G.-J. *J. Am. Chem. Soc.* **2006**, *128*, 8310–8319.
33. Li, B.; Kawatkar, S. P.; GeorgeS, S.; Strachan, H.; Woods, R. J.; Siriwardena, A.; Moremen, K. W.; Boons, G.-J. *Chembiochem* **2004**, *5*, 1127–1220.
34. Liu, H.; Sim, L.; Rose, D. R.; Pinto, B. M. *J. Org. Chem.* **2006**, *71*, 3007–3013.
35. Brunger, A. T.; Adams, P. D.; Clore, G. M.; DeLano, W. L.; Gros, P.; Grosse-Kunstleve, R. W.; Jiang, J. S.; Kuszewski, J.; Nilges, M.; Pannu, N. S.; Read, R. J.; Rice, L. M.; Simonson, T.; Warren, G. L. *Acta Crystallogr. D Biol. Crystallogr.* **1998**, *54*, 905–921.
36. Jones, T. A.; Zou, J. Y.; Cowan, S. W.; Kjeldgaard, M. *Acta Crystallogr. A* **1991**, *47*, 110–119.
37. Delano, W. L. The PyMOL Molecular Graphics System DeLano Scientific, San Carlos, CA, 2002.